sustainability

MDPI

Article

Optimization of the Process Parameters of Fully Mechanized Top-Coal Caving in Thick-Seam Coal Using BP Neural Networks

Minfu Liang [1,2], Chengjun Hu [3,4,*], Rui Yu [1,5], Lixin Wang [4], Baofu Zhao [4] and Ziyue Xu [1,*]

1 School of Mines, China University of Mining and Technology, Xuzhou 221116, China; liangmf2014@cumt.edu.cn (M.L.); LB19020006@cumt.edu.cn (R.Y.)
2 School of Economics and Management, China University of Mining and Technology, Xuzhou 221116, China
3 School of Energy and Mining Engineering, China University of Mining and Technology (Beijing), Beijing 100083, China
4 China Coal Tianjin Underground Engineering Intelligence Research Institute, Tianjin 561000, China; wanglixin@chinacoal.com (L.W.); zhaobaofu@chinacoal.com (B.Z.)
5 Wangjialing Coal Mine, China Coal Huajin Group Co., Ltd., Yuncheng 043000, China
* Correspondence: huchengjun@chinacoal.com (C.H.); TS20020060A31@cumt.edu.cn (Z.X.); Tel.: +86-185-2623-3835 (C.H.); +86-195-5225-1610 (Z.X.)

Abstract: The method of fully mechanized top-coal caving mining has become the main method of mining thick-seam coal. The process parameters of fully mechanized caving will affect the recovery rate and gangue content of top coal. Through numerical simulation software, the top-coal recovery rate and gangue content, under different fully mechanized caving process parameters, were simulated, and the influence law of different fully mechanized caving process parameters on top-coal recovery rate and gangue content was obtained. A decision model for top-coal caving process parameters was established with a BP neural network, and the optimal top-coal caving parameters were obtained for the actual situation of a working face. On this basis, a in-lab similarity simulation test of the particle material was carried out. The results show that the top-coal recovery rate and gangue content were 86.56% and 3.45%, respectively, and the coal caving effect was good. A BP neural network was used to study the decisions optimizing fully mechanized caving process parameters, which effectively improved the decision-making efficiency thereabout and provided a basis for realizing intelligent, fully mechanized caving mining.

Keywords: top-coal caving mining; process parameters; decision model; BP neural network; similarity simulation test

check for updates

Citation: Liang, M.; Hu, C.; Yu, R.; Wang, L.; Zhao, B.; Xu, Z. Optimization of the Process Parameters of Fully Mechanized Top-Coal Caving in Thick-Seam Coal Using BP Neural Networks. *Sustainability* **2022**, *14*, 1340. https://doi.org/10.3390/su14031340

Academic Editors: Longjun Dong, Yanlin Zhao and Wenxue Chen

Received: 31 December 2021
Accepted: 20 January 2022
Published: 25 January 2022

1. Introduction

The 'World Energy Statistics Review', released in 2020, shows that although global coal consumption has decreased, coal still accounts for about 27% of primary energy, which is still the main source of energy [1]. Especially for China, with its characteristic 'rich coal, lack of oil and less gas', the status of coal is unshakable. According to statistics, thick-seam coal accounts for 44% of the proven workable coal reserves in China, and nearly half of the coal consumption in China is provided by thick-seam coal mining [2,3].

Although the loads of hydraulic supports should be monitored in the process of fully mechanized top-coal caving mining to ensure continued safe production [4], this method has become the main strategy for thick-seam coal mining because of its low energy consumption, high output, strong geological adaptability and economic benefits [5–7]. It has gradually become the main method of thick-seam coal mining in China, Vietnam, Australia, Turkey and other countries [8–14]. Improving the recovery rates for top coal and reducing the gangue content of top coal are two key points in the study of fully mechanized caving mining techniques. Zhang NB et al. studied the influence of the arch formed by top coal and gangue on top-coal recovery rates and put forward the method of eliminating these arches to improve recovery rates [15]. Yasitli, NE and Unver B used the FLAC 3D software to simulate the top-coal caving process and granular, fine-sand materials in simulations thereof, and proposed that presplitting blasting technology could improve top-coal recovery rates [9,16]. Ghosh AK et al. believed that compressive strength, advance abutment pressure and top-coal seam thickness are important factors affecting top-coal recovery rates and proposed using the combination of blasting and vibration to destroy coal arches and thereby improve recovery rates [17], while Klishin VI and Klishin SV explored the relationship between the support opening sequence and the subsequent top-coal recovery rate [18,19].

However, there are few quantitative studies on the process parameters of fully mechanized caving mining. In recent years, thanks to rapid developments in science and technology, advanced artificial intelligence and machine learning algorithms have been increasingly applied to coal production [20–22]. Fan YJ et al. used a BP neural network to establish a safety evaluation model for coal mines and put forth an effective safety evaluation method for them [23]. Meng XZ et al. proposed an early warning method for coal mine safety, based on a BP neural network, that could effectively extract the characteristics of a coal mine's fault state and issue early warnings thereabout for coal mine safety [24]. The application of artificial neural networks provides a new scientific method for conducting research in the field of coal mining.

Therefore, this paper took the No. 12309 working face of the Wangjialing mine in Yuncheng City, Shanxi Province, China as its engineering background, adopting the research methods of numerical simulation, similarity simulation and BP neural networks to establish an optimization decision model of the process parameters for fully mechanized caving mining of thick-seam coal. So as to realize optimized decisions concerning the parameters for the fully mechanized caving mining technique in thick-seam coal mining, we obtained the optimal process parameters for such mining. Finally, we used them to improve mining and caving efficiency and the efficacy of coal caving.

2. Engineering Background

At the No. 12309 working face of the Wangjialing coal mine, which has adopted the fully mechanized, low-caving method of coal mining, its advancing length and width are 1320 m and 260 m, respectively. The buried depth of the main coal seam is about 400 m, its average thickness is 6.1 m, its dip angle is 2° and the hardness coefficient of its top coal is 1.8 ($f < 2$). There, the interlayer thickness is 0.2 m, the mining height is 3.1 m and the top-coal caving height is 3 m. Thus, the ratio of mining height to top-coal caving height is 1.03:1. The coal caving step is 0.865 m for one cutting with one caving. In the normal operation cycle, after each coal cutting, the tail beam is recovered and the coal opening is opened for coal caving operations. When the immediate top rock is discharged from the coal caving opening, the opening is closed, to stop coal caving. The first pressure step is 35 m, and the natural caving method is used to control the roof of the goaf. The properties of the roof and floor rock in the working face of the coal seam are shown in Figure 1, and the layout of the working face is shown in Figure 2.

The top coal falls from the working face in a relatively timely manner, generally, just after the top beam of the support. At the Wangjialing mine, the size of the lumpiness of top coal, mostly, is approximately 40 cm × 30 cm × 30 cm. Occasionally there are larger pieces, but they can all be released smoothly. Field observations of the top-coal caving process are shown in Figure 3.

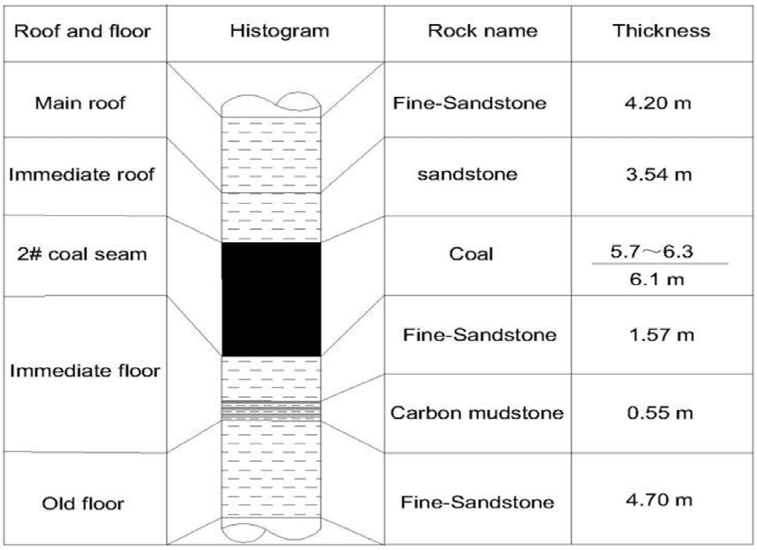

Figure 1. Comprehensive drilling histogram.

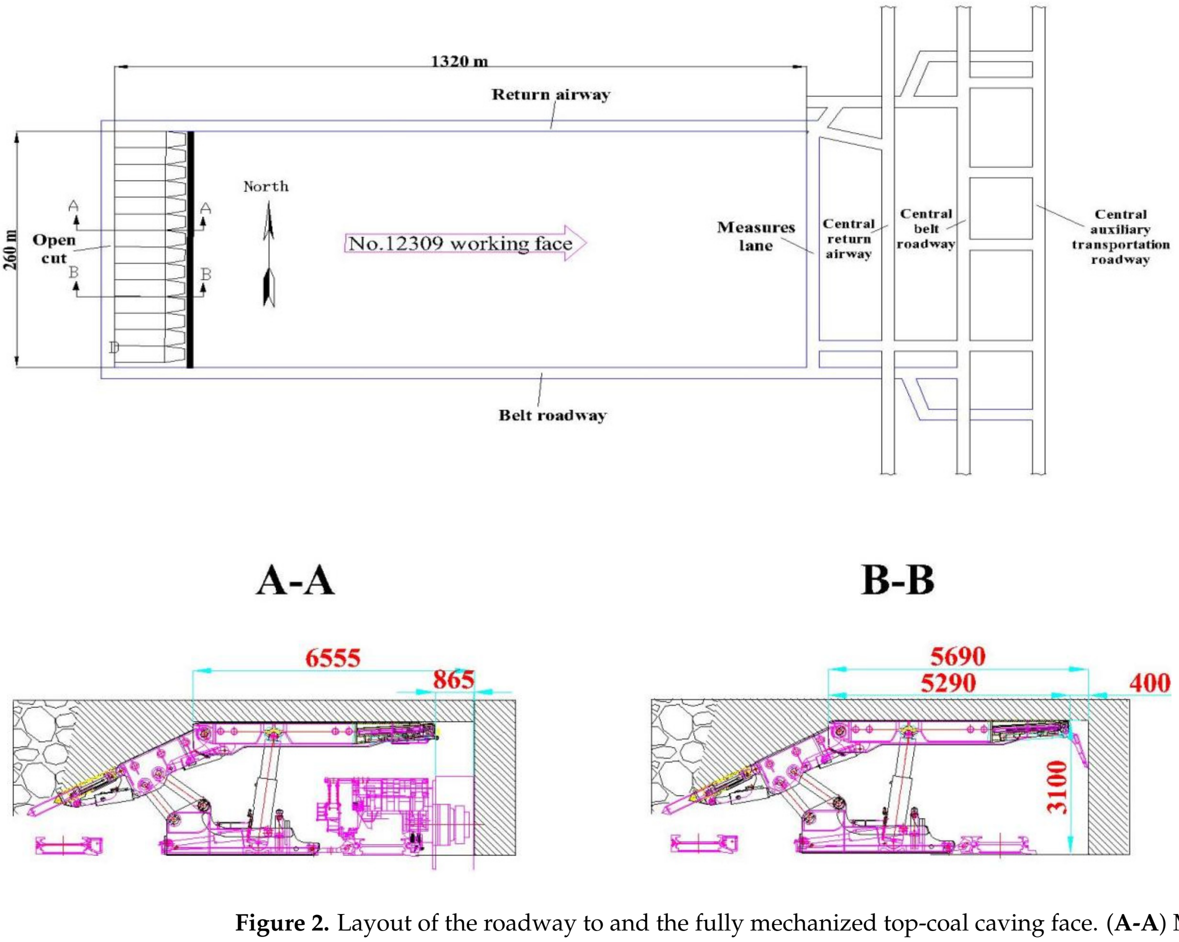

Figure 2. Layout of the roadway to and the fully mechanized top-coal caving face. (**A-A**) Maximum top control distance, (**B-B**) minimum top control distance.

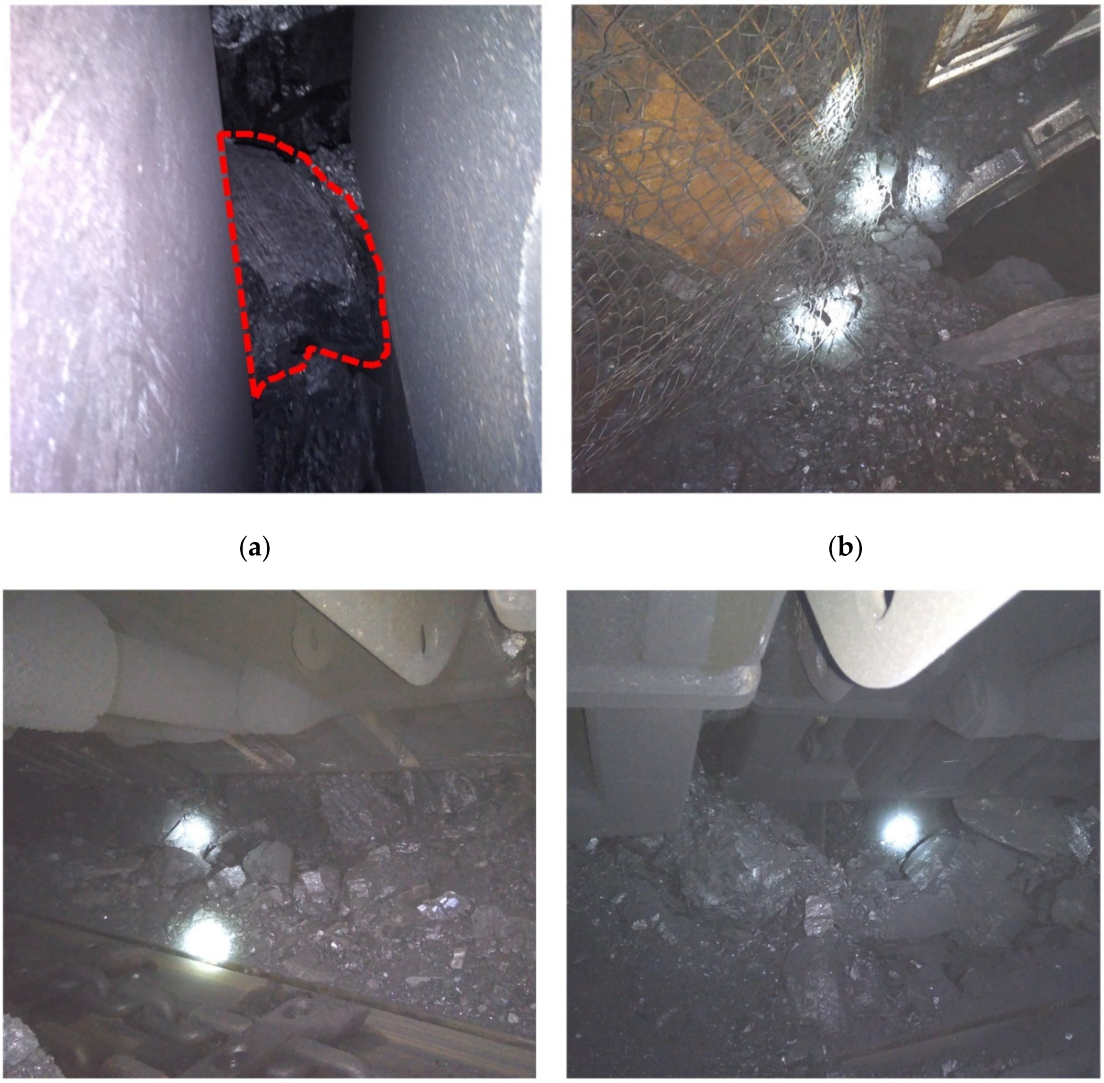

(a) (b) (c)

Figure 3. Top-coal caving condition of working face. (**a**) Broken top coal between supports; (**b**) coal caving at the top of the working face; (**c**) top-coal caving behind the conveyor at the front and rear of coal caving.

3. Methodology

3.1. Numerical Simulation Design

The two core indicators of the fully mechanized caving process are top-coal recovery rates and gangue content. Reasonable fully mechanized mining process parameters can effectively improve the top-coal recovery rates and reduce the gangue content. In order to study the influence of different fully mechanized caving process parameters on top-coal recovery rates and gangue content, the numerical simulation software PFC was used to conduct numerical simulation experiment schemes of different fully mechanized caving process parameters, with varying coal caving methods and procedures. The numerical simulation experiments of different fully mechanized top-coal caving process parameters were carried out by using the orthogonal experimental design method. By combining the principle of probability and statistics with computer technology, not only can the number of tests and calculation workload can be reduced, but the distribution of various influencing factors of fully mechanized top-coal caving mining is also more uniform within the test range, so as to achieve ideal results.

This numerical simulation study mainly focused on the top-coal releasing law without considering its crushing process. The top coal and immediate roof were assumed to be in a loose state. Therefore, both top coal and immediate roof adopted a linear constitutive model for 'Ball–Ball' and 'Ball–Facet' connections in numerical simulations. The elastic model was adopted for the bottom coal and main roof, and the linear contact model was adopted for each part and its internal contact model. The buried depth of the main coal seam was 400 m and the height of the numerical model was 18.84 m. Therefore, in the process of initial balance simulation, the weight of the 381.16 m-thick rock stratum should be applied to the upper surface of the model, and the average unit weight of the rock stratum was 25 KN/m^3, such that a boundary stress of σ_z = 9.529 MP was applied to the upper boundary of the model. Rigid walls slightly larger than the model were set up at the front, rear, left, right and bottom of the model, and its velocity was fixed at 0 m/s to server as a displacement boundary. The contact parameters are shown in Table 1, and the unit parameters are shown in Table 2.

Table 1. Contact parameters.

Contact Type	Constitutive Model	Firc	dp_Nratio	dp_Sratio	kn	ks
Immediate roof	Liner	0.5	0.3	0.3	4×10^8	4×10^8
Top coal		0.4	0.3	0.3	3×10^8	3×10^8
Ball–Ball		0.4	0.3	0.3	3×10^8	3×10^8
Ball–Facets		0.3	0.3	0.3	5×10^8	5×10^8

Table 2. Unit parameters.

Rock Stratum	Unit Type	Elastic Modulus/GPa	Bulk Density/kg·m^{-3}	Poisson's Ratio	Local Damping
Main roof	Zone	15.0	2660	0.34	/
Immediate roof	Ball	13.6	2660	/	0.7
Top coal	Ball	2.3	1400	/	0.7
Bottom coal	Zone	2.3	1400	0.26	/

The numerical simulation schemes of different fully mechanized caving process parameters with varying coal caving methods have considered various factors, such as coal seam thickness, mining and caving ratio, number of coal caving rounds, coal caving sequence, number of coal caving openings and top-coal particle size. Each factor was divided into three levels, as shown in Table 3. According to the orthogonal test method, a total of 18 models were established, and the numerical simulation schemes are shown in Table 4. The numbers 1, 2 and 3 in Table 4 refer to the corresponding factor level in Table 3.

The factors considered in the numerical simulation schemes of different fully mechanized top-coal caving process parameters with varying coal caving procedures include coal seam thickness, mining and caving ratio, coal caving procedure and top-coal particle size. Each factor was divided into three levels, as shown in Table 5. According to the orthogonal test method, a total of 9 models were established, and the numerical simulation schemes are shown in Table 6. The numbers 1, 2 and 3 in Table 6 correspond to the corresponding factor level in Table 5.

Table 3. Factor levels for the coal caving method.

Level	Coal Seam Thickness (m)	Caving Ratio	Number of Coal Caving Rounds	Coal Caving Sequence	Number of Coal Discharge Openings at the Same Time	Top-Coal Particle Size (m)
1	6	1:1	Single round	Sequential	Single opening	0.15–0.3
2	8	1:1.5	Two rounds	Group interval	Two openings	0.25–0.4
3	10	1:2	Three rounds	Interval return	Three openings	0.35–0.5

Table 4. Orthogonal simulation schemes for coal caving method.

Scheme No	Coal Seam Thickness	Caving Ratio	Number of Coal Caving Rounds	Coal Caving Sequence	Number of Coal Discharge Openings	Top-Coal Particle Size
1	1	1	1	1	1	1
2	1	2	2	2	2	2
3	1	3	3	3	3	3
4	2	1	1	2	2	3
5	2	2	2	3	3	1
6	2	3	3	1	1	2
7	3	1	2	1	3	2
8	3	2	3	2	1	3
9	3	3	1	3	2	1
10	1	1	3	3	2	2
11	1	2	1	1	3	3
12	1	3	2	2	1	1
13	2	1	2	3	1	3
14	2	2	3	1	2	1
15	2	3	1	2	3	2
16	3	1	3	2	3	1
17	3	2	1	3	1	2
18	3	3	2	1	2	3

Table 5. Factor levels for the coal caving procedure.

Level	Coal Seam Thickness (m)	Caving Ratio	Coal Caving Procedure	Top-Coal Particle Size (m)
1	6	1:1	One cutting with one caving	0.15–0.3
2	8	1:1.5	Two cutting with one caving	0.25–0.4
3	10	1:2	Three cutting with one caving	0.35–0.5

Table 6. Orthogonal simulation schemes for coal caving procedure.

Scheme No	Coal Seam Thickness	Caving Ratio	Coal Caving Procedure	Top-Coal Particle Size
1	1	1	1	1
2	1	2	2	2
3	1	3	3	3
4	2	1	2	3
5	2	2	3	1
6	2	3	1	2
7	3	1	3	2
8	3	2	1	3
9	3	3	2	1

3.2. Numerical Simulation Calculation

3.2.1. BP Neural Network

The artificial neural network is a nonlinear and adaptive information processing system composed of a large number of standardized neurons, which is capable of simulating a biological neural network, and it has been deeply studied and widely used all over the world [25]. At the same time, due to the different connections of artificial neurons, a variety of artificial neural network models have been developed. Among them, the BP neural network is the most widely used model in artificial neural networks, which is a multi-layer feedforward neural network trained according to the algorithm of error back propagation [26]. The BP neural network is composed of an input layer, hidden layer and output layer and based on Sigmod function for operation and application, and has a strong nonlinear mapping ability and flexible network results [27]. Therefore, we can establish a nonlinear evaluation model by using this technology to better solve the randomness of weight definition, and ensure the accuracy and scientificity of evaluation results and activities [28,29].

The neural network program was developed using Matlab platform; the program flow is as follows:

- Loading initialized training sample parameters, input array P and output array A, and randomly selecting 80% of the samples as the training group (P1, A1) and 20% of the samples as the test group (P2, A2).
- Defining a series of neuron parameters such as the number of neural network layers, the number of neurons per layer, the maximum number of trainings (net.trainParam.epochs) and the training target error (net.trainParam.goal).
- Using the feedforwardnet function in Matlab to establish the neuron model, and using the train function to train the input and output array of the samples, such that a corresponding network is obtained.
- Using the Sim function to calculate the error between the input data P2 of the verification group and the output A2 of the verification group in the network. According to the error condition, returning to the second step to adjust the neural network parameters and continuing to train until the error requirements are met.
- Taking the target parameters into the Sim function, calculating the output of the neural network net, the predicted results of the target parameters are obtained.

3.2.2. Cross-Validation

Cross-validation can obtain as much effective information as possible from limited learning data, so as to obtain more appropriate two-layer weights. Additionally, this method learns samples from multiple directions, which can effectively avoid falling into local minima. Dong L et al. [30] established a microseismic event and blasting event identification model based on a convolutional neural network by using cross-validation. The collected microseismic and blasting event waveforms were composed of a training set, test set and verification set, respectively. Compared with other machine learning methods, this method has high identification accuracy. In addition, Dong L et al. [31] proposed the LM-CAG-CDR method and recommended 16 combined methods to evaluate the level of clean and safe production of phosphate rock, which improved the development level of the clean and safe mining of phosphate rock.

In order to verify the effectiveness of the BP neural network, the parameter design and simulation results of 18 orthogonal experimental models described above were used as samples to train the BP neural network and obtain a neural network model (14 models as training set and 4 models as test set). The objective laws hidden beneath the orthogonal test samples can be discovered, the coal caving rates and gangue content of all mining conditions and fully mechanized top-coal caving process combinations can be predicted without numerical simulation (a total of 729 combinations were used as the verification set), and the effectiveness of the neural network program can be verified with reference to the analysis of the numerical simulation results.

3.2.3. Optimized Decision

Based on the function and characteristics of the BP neural network, an optimized decision-making model for top-coal caving mining process parameters based on the BP neural network was established. The model could make decisions on top-coal caving mining process parameters according to the actual mining conditions of the coal mine, and obtain the optimal mining process parameters.

According to the actual situation of the mine, the input vector P was the natural factors affecting the mining and recovery rates of top coal, mainly including the average thickness of coal seam X1 (m), firmness coefficient of top coal X2, development degree of interlayer joint fracture X3, buried depth X4 (m), lithology and thickness of coal seam roof X5, and dip angle of coal seam X6 (°). The output process parameters of top-coal caving mainly included coal caving sequence Y1, mining to caving ratio Y2, and coal caving step Y3 (m). In order to make the decisions on top-coal caving process parameters more universal, the conceptual description in input and output was numerically processed based on the geological and process parameters of working faces in multiple coal mines. The processing results are shown in Table 7.

Table 7. Learning samples.

Sample Parameter	Concept Description	Neural Network Assignment Range
Interlayer and joint fracture development degree	Interlayer thickness > 0.5 m, Joint fissure less developed	0–0.33
	Interlayer thickness 0.2–0.5 m Joint fracture development general	0.34–0.66
	Interlayer thickness < 0.2 m Joint fracture development	0.67–1.0
Roof lithology and thickness	Pressure step < 25 m Immediate roof thickness > 10 m	0.75–1.0
	Pressure step 25–50 m Immediate roof thickness 5–10 m	0.5–0.75
	Pressure step 25–50 m Immediate roof thickness < 5 m	0.25–0.49
	pressure step > 50 m Immediate roof thickness < 3 m	0–0.24
Coal caving sequence	Multi-round sequential coal caving	0.76–1.0
	Interval caving coal among multi-cutting	0.51–0.75
	Single-round sequential coal caving	0.26–0.50
	Single round interval coal caving	0–0.25

A 6-layer neural network was established, with 10 neurons, 6 input parameters and 3 output parameters in each layer, as shown in Figure 4. The three output parameters were the optimized process parameters.

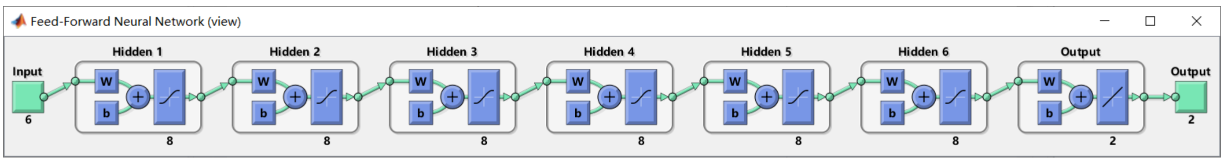

Figure 4. Parameters prediction neural network diagram.

3.3. Similarity Simulation Test

According to the geological conditions of the No. 12309 working face of the Wangjialing coal mine and the determined optimal fully mechanized top-coal caving process parameters, the similarity simulation test system for top-coal caving was designed and tested in the laboratory. The model frame was 2000 mm in length, 200 mm in width and 2500 mm in height, and the simulated material was composed of sand, lime and Bali stone. The height of the laid simulation material was 130.5 cm, and the geometric similarity ratio of the simulation experiment was C = 30/318 = 1: 10.6. According to the field observation, the top coal is easy to release, and there are few cases of large coal blocking. Therefore, the top coal, immediate roof and main roof in the experiment were laid into loose bodies, the coal seam was simulated by black particles, and the immediate roof was simulated by white particles. The similar material simulation test bench is shown in Figure 5, and the particle arrangement position is shown in Figure 6. The top coal was divided into upper, middle and lower layers by using marker particles. A 10 MPa uniformly distributed load was applied on the top layer of the model to simulate the load on the actual rock stratum (calculated according to the buried depth of 400 m). The opening and closing of the coal discharge opening were simulated by pulling out and pushing in the separator plate interposed between the supports, and the coal discharging was started and stopped under the action of the load.

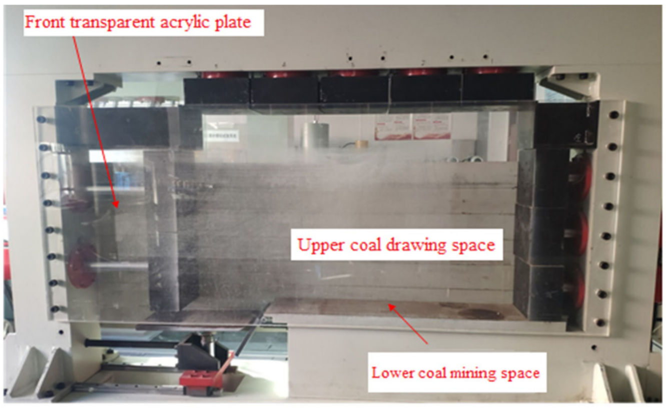

Figure 5. Similar material simulation test bench.

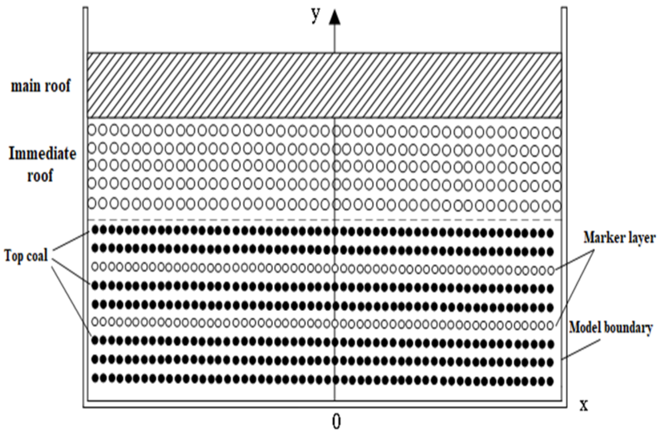

Figure 6. Diagram of particle position arrangement.

4. Results and Discussion

4.1. Numerical Simulation Experiment

4.1.1. Coal Caving Mode

The coal caving method mainly included three methods: sequential coal caving, grouping interval and interval return coal caving. The description with respect to Figures 7–9 is as follows: the coal–gangue boundary refers to the boundary between the top coal and the immediate roof; that is, the green particles represent the immediate roof and the blue particles represent the top coal. Residual coal refers to the part of coal left after top-coal caving.

(1) Sequential coal caving

In order to study the flow characteristics of top coal under different simulation schemes, the representative scheme of the six numerical simulation schemes was selected for analysis, namely Scheme 1 in Table 4. The simulation process is shown in Figure 7.

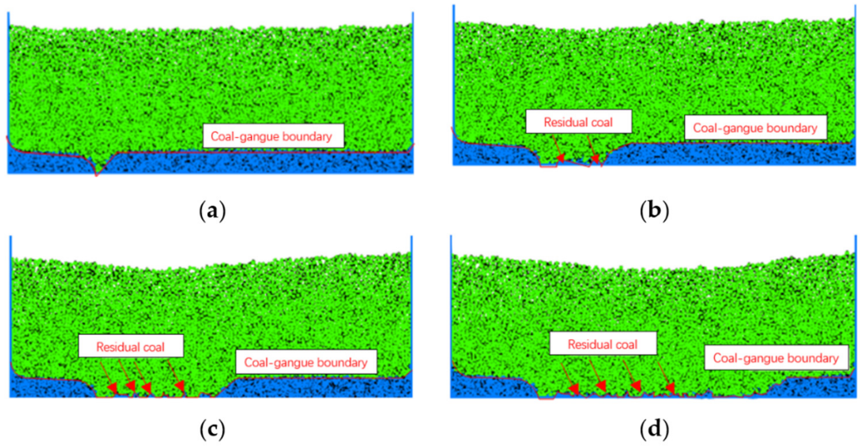

Figure 7. Simulation scheme 1 top-coal flow process diagram. (**a**) The 1# support coal caving end; (**b**) 7# support coal caving end; (**c**) 10# support coal caving end; (**d**) all supports finished.

The geological conditions and process parameters for simulation scheme 1 are as follows: the thickness of the coal seam is 6 m, the mining to caving ratio is 1:1 (mining height is 3 m, caving height is 3 m), single-round sequential coal caving, the number of caving openings is 1, and the particle size of top coal is 0.15~0.3 m. After the upper coal above 1# support is released, there is an obvious funnel-shaped caving space above the support (Figure 7a). When the support top coal was released in sequence, the boundary of the coal gangue dropped gently. After discharging all of the coal, the top-coal recovery rate and gangue content were 90.72% and 2.72%, respectively. Therefore, a single round of sequential caving could achieve a better caving effect for a short top-coal caving height.

(2) Group interval coal caving

Six representative numerical simulation schemes with coal caving sequence 2 were selected for analysis, namely Scheme 8 in Table 4. The simulation process is shown in Figure 8.

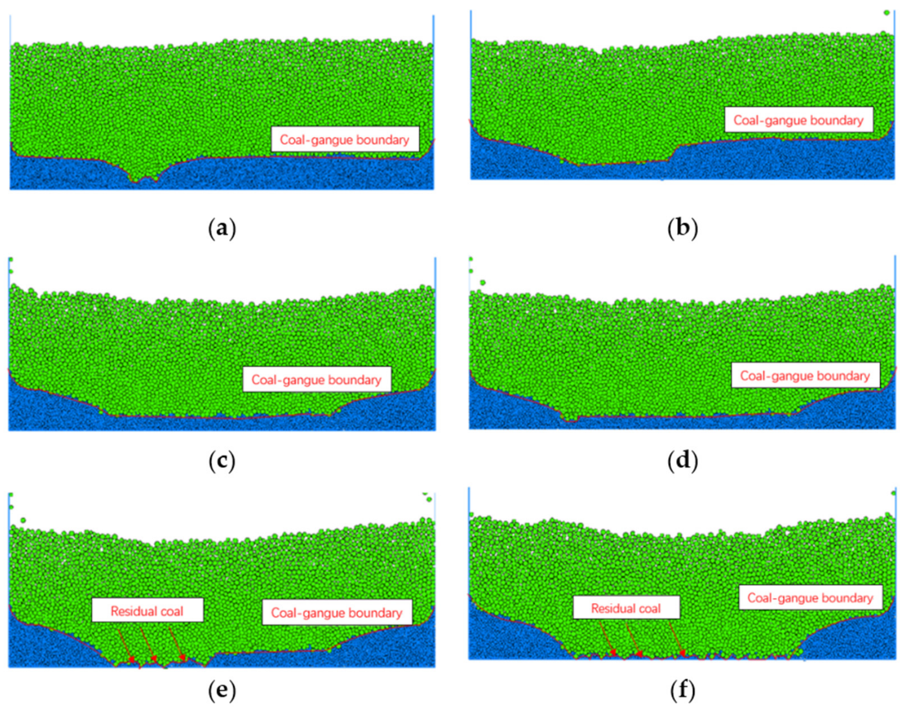

Figure 8. Simulation scheme 8 top-coal flow process diagram. (**a**) The 1# support coal caving end; (**b**) 10# support coal caving end; (**c**) end of the first round of coal caving; (**d**) 1# support end of second coal caving; (**e**) 10# support end of second coal caving; (**f**) end of the second round of coal caving.

Geological conditions and process parameters of simulation program 8: coal seam thickness 10 m, mining to caving ratio 1:1.5 (mining height 4 m, caving height 6 m), multi-round interval caving, the number of caving openings is 1, and the particle size of top coal is 0.35~0.5 m. Due to the use of multiple rounds of coal caving, the boundary between coal and gangue in the first round of coal caving decreased evenly (Figure 8a–c), preventing gangue from mixing into adjacent coal caving openings in advance. When the remaining top coal above the support continued to cave out, the flow characteristics of top coal were similar to those of simulation scheme 1 (caving height 3 m) due to the thin thickness of the remaining top coal. After all the supports were placed, there was less top coal missing in the goaf (Figure 8d–f). The top-coal recovery rate and gangue content were 91.88% and 4.05%, respectively. The coal caving effect was good. Thus, when the top-coal caving height is large (6 m), multiple rounds of coal caving should be adopted to ensure the uniform descent of the coal-gangue boundary and to prevent the gangue above the coal caving support from entering the adjacent coal caving opening too early.

(3) Interval return coal caving

Six representative numerical simulation schemes with coal caving sequence 3 were selected for analysis, namely scheme 13 in Table 4. The simulation process is shown in Figure 9.

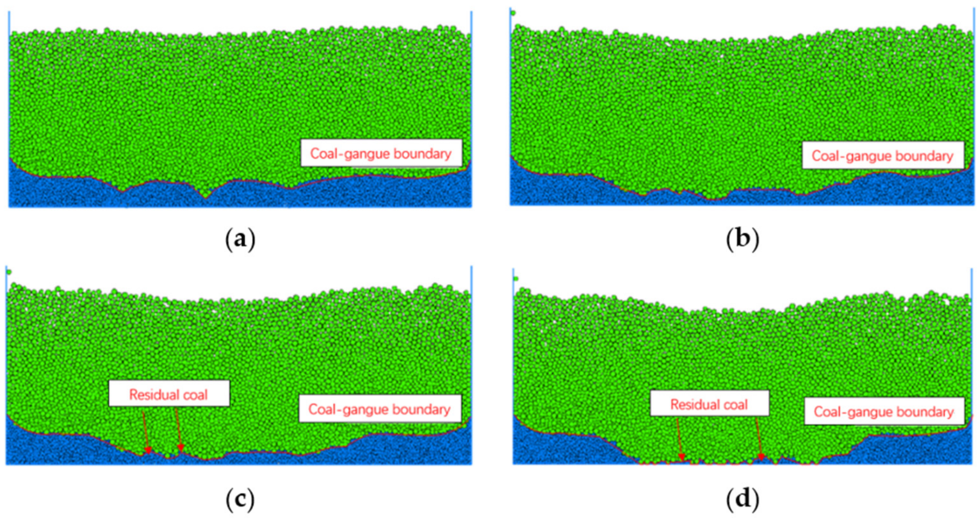

Figure 9. Simulation scheme 8 top-coal flow process diagram. (**a**) The 2# support end of first coal caving; (**b**) end of the first round of coal caving; (**c**) 2# support end of second coal caving; (**d**) end of the second round of coal caving.

The geological conditions and process parameters of simulation scheme 13 are as follows: coal seam thickness is 8 m, mining to caving ratio is 1:1 (mining height is 4 m, caving height is 4 m), the number of caving openings is 1, and the top-coal particle size is 0.35~0.5 m. Due to using group interval caving, the boundary line of coal and gangue descends unevenly after the first round of caving (Figure 9a,b), and the remaining top coal thickness is obviously different. There is more top coal left in the goaf after the second round of coal caving with all supports (Figure 9c,d). The top-coal caving rate and gangue content were 85.77% and 2.72%, respectively. In addition, compared with scheme 5 with the same coal thickness, the caving ratio (1:1) of scheme 13 was greater than that of scheme 5 (1:1.5), and the top-coal recovery rate of scheme 13 was better than that of scheme 5. Consequently, choosing a smaller caving ratio is conducive to top-coal caving under the condition of the same coal thickness.

The top-coal recovery rate and gangue content of different simulation schemes with varying coal caving methods were counted, as shown in Figure 10. Through the analysis of the 18 coal caving schemes, the top-coal recovery rate ranges from 73.43% to 95.41%, and the gangue content ranges from 1.09 to 10.21%. The difference for top-coal recovery rate and gangue content is obvious when adopting different coal caving sequences and different process parameters. Therefore, in order to obtain the ideal top-coal caving effect, the top-coal caving sequence and process under specific geological production conditions need to be analyzed. In addition, if schemes 7 and 11 are ignored, there is a positive correlation between the top-coal recovery rate and the gangue content. That is, with the increase in gangue content, the top coal release rate will also increase accordingly. On the other hand, as the gangue content decreases, the top-coal recovery rate will also decrease. Hence, properly increasing the gangue content could improve the top-coal recovery rate, and the critical point for gangue content needs to be determined according to the specific coal caving process parameters and actual production situation.

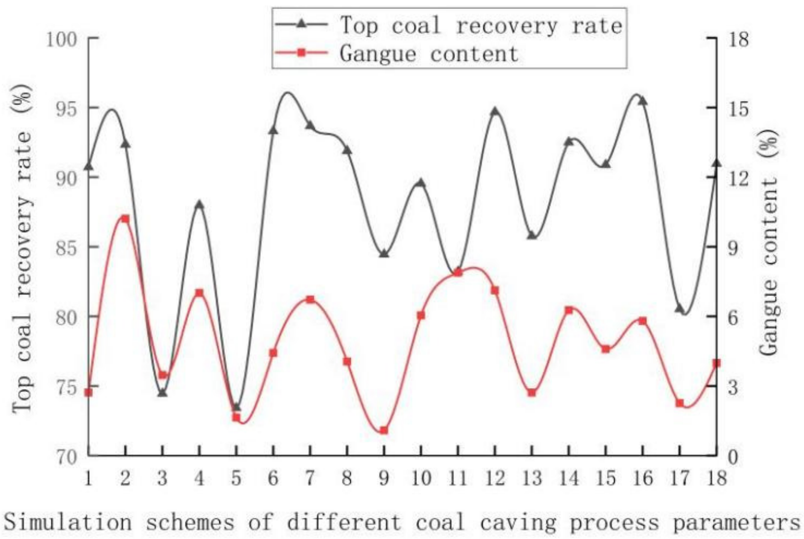

Figure 10. Top-coal recovery rate and gangue content curves.

4.1.2. Coal Caving Procedure

According to Tables 3 and 4, different simulation schemes with varying coal caving procedures were simulated. The top-coal recovery rate and gangue content of different simulation schemes were counted, as shown in Figure 11. The top-coal recovery rate ranged from 71.52% to 92.59% and gangue content ranged from 1.79% to 8.08%, respectively. There are great differences in top-coal recovery rate and gangue content when adopting different coal caving procedures and different process parameters. Consequently, in view of specific geological production conditions, in order to obtain an ideal coal caving effect, the coal caving step and coal caving procedure should be considered in detail. In addition, if scheme 4 is neglected, there is also a positive correlation between the top-coal recovery rate and the gangue content. That is, with the increase in gangue content, the top-coal recovery rate will also increase accordingly. On the other hand, as the gangue content decreases, the top-coal recovery rate will also decrease. When the coal caving step was taken as a single variable, it was found that with the increase in coal caving step, the top-coal recovery rate decreased and the gangue content increased; as the coal caving step decreased, the top-coal recovery rate increased and the gangue content decreased. Therefore, selecting a small caving step and appropriately increasing the gangue content could improve the top-coal recovery rate, and the critical point for gangue content needs to be determined according to specific caving process parameters and actual production conditions.

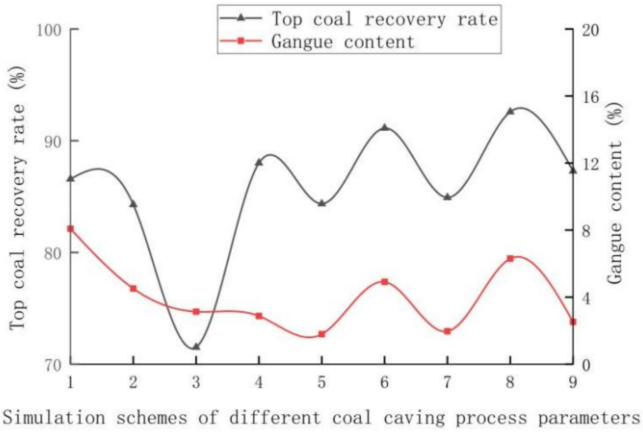

Figure 11. Top-coal recovery rate and gangue content curves.

4.2. Cross-Validation Results

All 729 possible model parameter combinations were input into the trained neural network model, and the optimized coal caving process parameters under different coal caving modes were obtained after ranking according to the comprehensive evaluation indexes, as shown in Table 8. The effectiveness of the BP neural network was verified.

Table 8. Optimized top-coal caving process parameters under different top-coal caving modes.

Parameters	Coal Seam Thickness	Caving Ratio	Number of Coal Caving Rounds	Coal Caving Order	Number of Coal Caving Openings	Top-Coal Particle Size	Top-Coal Recovery Rate	Gangue Content
Input parameters	1	1	0.5	0.5	0.5	0.25	92.48%	2.16%
Actual parameters	10 m	1:1	Three rounds	Three ports	Interval return coal caving	0.15–0.3 m	/	/

4.3. Optimized Process Parameters

According to the occurrence conditions of the coal seam in the Wangjialing coal mine, the main parameters of the Wangjialing coal mine were brought into the decision-making model (Figure 4) to obtain the decision-making process parameters thereof, as shown in Table 9. The optimized technological parameters for fully mechanized mining in the Wangjialing coal mine were single-round sequential coal caving, mining and caving ratio 1.09:1, and coal caving step distance 0.78 m.

Table 9. Determination of fully mechanized caving process parameters.

Coal Seam Occurrence Conditions (X)		Optimized Process Parameter (Y)	
Coal seam thickness (X1)	6.1 m	Coal caving sequence	Single-round sequential
Top-coal firmness coefficient (X2)	1.8		
Interlayer and joint fissure (X3)	0.4	Caving ratio	1.09
Depth of embedment (X4)	400 m		
Roof lithology and thickness (X5)	0.4	Coal caving step	0.78 m
Top-coal dip angle (X6)	2°		

4.4. Coal Caving Effectiveness

Figure 12 shows the experimental process of single-round sequential coal caving. Additionally, Table 10 shows the top-coal recovery rate and gangue content for each coal caving opening in single-round sequential coal caving.

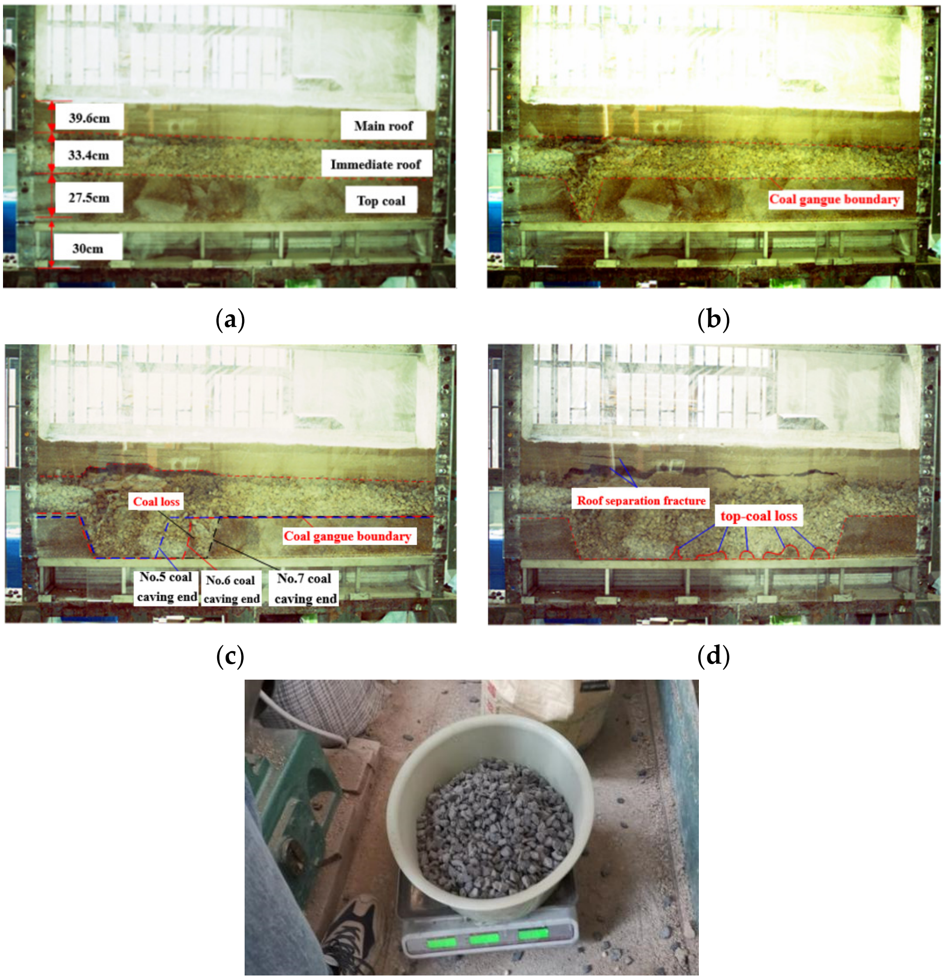

(**a**) (**b**) (**c**) (**d**) (**e**)

Figure 12. Single-round sequential coal caving process. (**a**) Initial state; (**b**) No. 3 coal caving end; (**c**) No. 5~7 coal caving end; (**d**) end of coal caving; (**e**) weighing the released coal.

Table 10. Single-round sequential coal caving results.

Coal Caving Opening Number	3	4	5	6	7	8	9	10	11	12	13	Sum
Coal quantity (kg)	2.82	2.82	2.82	2.82	2.82	2.82	2.82	2.82	2.82	2.82	2.82	31.02
Coal output (kg)	2.83	2.45	2.43	2.44	2.37	2.38	2.32	2.45	2.32	2.44	2.42	26.85
Gangue output (kg)	0.11	0.2	0.21	0.05	0.12	0.1	0.03	0.02	0.03	0.08	0.12	1.07
Top-coal recovery rate (%)	100.35	86.88	86.17	86.52	84.04	84.40	82.27	86.88	82.27	86.52	85.82	86.56
Gangue content (%)	3.90	7.09	7.45	1.77	4.98	4.26	1.06	0.71	1.06	2.84	4.26	3.45

Analysis of Figure 12 and Table 9 shows that the similarity simulation results of single-round sequential caving in the No. 12309 working face of the Wangjialing coal mine are consistent with the results of numerical simulations. When the top-coal caving height was small, the single-round sequential coal caving could achieve a better coal caving effect. When the first support (3# support) carried out coal caving, there was an obvious funnel-shaped coal caving space above the support (Figure 12b). When the top coal of the caving support was caved out sequentially, the coal gangue boundary descended gently; only a small part of top coal was left after caving all of the coal (Figure 12d). The top-coal recovery rate was 86.56% and the gangue content was 3.45%, with good caving effect. Thus, compared with the analysis and decision making of process parameters through industrial experiments, which takes a lot of time and consumes a certain amount of manpower and material resources, using the BP neural network to optimize the decision-making process of fully mechanized caving process parameters can effectively improve the decision-making efficiency and provide a basis for the realization of intelligent, fully mechanized caving mining.

5. Conclusions

In this study, the effects of different fully mechanized top-coal caving process parameters with different caving methods and different caving procedures on top-coal recovery rates and gangue content were studied. According to the occurrence conditions and actual production situation of the Wangjialing coal mine, the decision-making model for fully mechanized top-coal caving mining process parameters was established by using the BP neural network, and the optimized fully mechanized top-coal caving process parameters of Wangjialing coal mine were obtained. The in-lab similarity simulation experiment was carried out to verify the coal caving effect of the optimized fully mechanized top-coal caving process parameters. The following conclusions were drawn from the whole process:

(1) For different coal caving process parameters, the top-coal recovery rates and gangue content are obviously differen, the top-coal recovery rate could be improved by appropriately increasing the gangue content, and the critical point for the gangue content should be determined according to the specific coal caving process parameters and the actual production situation.
(2) In top-coal caving mining, the selection of a small caving step distance was conducive to top-coal caving.When the top-coal caving height was small, a better coal caving effect could be achieved by single-round sequential coal caving.When the top-coal caving height was large (6 m), using multiple rounds of coal caving was conducive to ensuring that the boundary between coal and gangue dropped evenly, and preventing the gangue above the coal caving support from entering the adjacent coal caving opening prematurely.
(3) Through the in-lab similar simulation experiment, it was indicated that the BP neural network can be used to study the optimized decision making of mining process parameters and can obtain good results, improving the benefit of process parameter decision making, and provide the basis for realizing the intelligent mining of fully mechanized top-coal caving.
(4) There are many factors affecting the top-coal recovery rate and gangue content in addition to the fully mechanized caving process parameters studied in this paper. The calculation of a relaxed ellipsoid can also be considered in future research.

Author Contributions: M.L., C.H., R.Y. and L.W. designed the study and experiment; C.H., B.Z. and Z.X. collected the data; C.H., R.Y., L.W. and Z.X. conducted the data analysis; R.Y., L.W. and B.Z. provided the statistical methods; M.L., C.H., R.Y. and Z.X. drafted the paper; M.L., C.H., R.Y. and Z.X. edited the paper. All authors have read and agreed to the published version of the manuscript.

Funding: This research was funded by the National Natural Science Foundation of China (Nos. 52004273 and 51874276), the Natural Science Foundation of Jiangsu Province (No. BK20200639), the China Postdoctoral Science Foundation (No. 2019M661992) and the Fundamental Research Funds for the Central Universities (No. 2020QN38).

Institutional Review Board Statement: Not applicable.

Informed Consent Statement: Not applicable.

Data Availability Statement: All data and code used or analyzed in this study are available from the corresponding author on reasonable request.

Acknowledgments: The authors thank the editor and three anonymous reviewers of the paper. Their constructive suggestions and comments have considerably improved the quality of the paper.

Conflicts of Interest: The authors declare no conflict of interest.

References

1. Leonard, M.D.; Michaelides, E.E.; Michaelides, D.N. Substitution of coal power plants with renewable energy sources—Shift of the power demand and energy storage. *Energy Convers. Manag.* **2018**, *164*, 27–35. [CrossRef]
2. Wang, J.; Yu, B.; Kang, H.; Wang, G.; Mao, D.; Liang, Y.; Jiang, P. Key technologies and equipment for a fully mechanized top-coal caving operation with a large mining height at ultra-thick coal seams. *Int. J. Coal Sci. Technol.* **2015**, *2*, 97–161. [CrossRef]
3. Bhattacharya, M.; Rafiq, S.; Bhattacharya, S. The role of technology on the dynamics of coal consumption–economic growth: New evidence from China. *Appl. Energy* **2015**, *154*, 686–695. [CrossRef]
4. Herezy, Ł.; Janik, D.; Skrzypkowski, K. Powered Roof Support—Rock Strata Interactions on the Example of an Automated Coal Plough System. *Studia Geotech. Mech.* **2018**, *40*, 46–55. [CrossRef]
5. Wang, Z.; Zhang, G.; Zhao, L. Recognition of rock–coal interface in top coal caving through tail beam vibrations by using stacked sparse autoencoders. *J. Vibroeng.* **2016**, *18*, 4261–4275. [CrossRef]
6. Wu, J.; Qin, Y.; Zhai, M. Mining safety of longwall top-coal caving in China. In Proceedings of the 8th U.S. Mine Ventilation Symposium, Rolla, MO, USA, 11–17 June 1999.
7. Wang, J. Development and prospect on fully mechanized mining in Chinese coal mines. *J. Coal Sci. Eng.* **2014**, *1*, 253–260. [CrossRef]
8. Le, T.D.; Mitra, R.; Oh, J.; Hebblewhite, B. A review of cavability evaluation in longwall top coal caving. *Int. J. Min. Sci. Technol.* **2017**, *27*, 907–915. [CrossRef]
9. Yasitli, N.E.; Unver, B. 3D numerical modeling of longwall mining with top-coal caving. *Int. J. Rock Mech. Min. Sci.* **2005**, *42*, 219–235. [CrossRef]
10. Alehossein, H.; Poulsen, B.A. Stress analysis of longwall top coal caving. *Int. J. Rock Mech. Min. Sci.* **2010**, *47*, 30–41. [CrossRef]
11. Si, G.; Jamnikar, S.; Lazar, J.; Shi, J.Q.; Durucan, S.; Korre, A.; Zavšek, S. Monitoring and modelling of gas dynamics in multi-level longwall top coal caving of ultra-thick coal seams, part I: Borehole measurements and a conceptual model for gas emission zones. *Int. J. Coal Geol.* **2015**, *144–145*, 98–110. [CrossRef]
12. Klishin, V.; Nikitenko, S.; Opruk, G. Longwall top coal caving (LTCC) mining technologies with roof softening by hydraulic fracturing method. *IOP Conf. Ser. Mater. Sci. Eng.* **2018**, *354*, 012015. [CrossRef]
13. Klishin, V.I.; Fryanov, V.N.; Pavlova, L.D.; Opruk, G.Y. Modeling top coal disintegration in thick seams in longwall top coal caving. *J. Min. Sci.* **2019**, *55*, 247–256. [CrossRef]
14. Ti, Z.; Li, J.; Wang, M.; Wang, K.; Jin, Z.; Tai, C. Fracture mechanism in overlying strata during longwall mining. *Shock. Vib.* **2021**, *2021*, 4764732. [CrossRef]
15. Zhang, N.; Liu, C.; Wu, X.; Ren, T. Dynamic Random Arching in the Flow Field of Top-Coal Caving Mining. *Energies* **2018**, *11*, 1106. [CrossRef]
16. Unver, B.; Yasitli, N.E. Modelling of strata movement with a special reference to caving mechanism in thick seam coal mining. *Int. J. Coal Geol.* **2006**, *66*, 227–252. [CrossRef]
17. Ghosh, A.K.; Gong, Y. Improving coal recovery from longwall top coal caving. *J. Mines Met. Fuels* **2014**, *62*, 51–64.
18. Klishin, V.I.; Klishin, S.V. Coal extraction from thick flat and steep beds. *J. Min. Sci.* **2010**, *46*, 149–159. [CrossRef]
19. Klishin, S.V.; Klishin, V.I.; Opruk, G.Y. Modeling coal discharge in mechanized steep and thick coal mining. *J. Min. Sci.* **2013**, *49*, 932–940. [CrossRef]
20. Yu, K.; Qiang, W. Application of ant colony clustering algorithm in coal mine gas accident analysis under the background of big data research. *J. Intell. Fuzzy Syst.* **2020**, *38*, 1381–1390. [CrossRef]
21. Ruilin, Z.; Lowndes, I. The application of a coupled artificial neural network and fault tree analysis model to predict coal and gas outbursts. *Int. J. Coal Geol.* **2010**, *84*, 141–152. [CrossRef]
22. Jiang, H.; Song, Q.; Gao, K.; Song, Q.; Zhao, X. Rule-based expert system to assess caving output ratio in top coal caving. *PLoS ONE* **2020**, *15*, e0238138. [CrossRef] [PubMed]
23. Fan, S. Study of the Safety Assessment Model of Coal Mine Based on BP Neural Network. In Proceedings of the International Conference on Intelligent Computation Technology & Automation IEEE, Changsha, China, 10–11 October 2009.
24. Meng, X.; Lu, P.; Wang, B. Coal mine safety warning system based on principal component method and neural network. In Proceedings of the 2017 6th Data Driven Control and Learning Systems (DDCLS) IEEE, Chongqing, China, 26–27 May 2017.
25. O'Rourke, D.; Ringer, A. The impact of sustainability information on consumer decision making. *J. Ind. Ecol.* **2015**, *20*, 882–892. [CrossRef]
26. Treichler, E.B.H.; William, D. Beyond shared decision-making: Collaboration in the age of recovery from serious mental illness. *Am. J. Orthopsychiatry* **2017**, *87*, 567–574. [CrossRef] [PubMed]
27. Li, W. Consumer Decision-Making Power Based on BP Neural Network and Fuzzy Mathematical Model. *Wirel. Commun. Mob. Comput.* **2021**, *2021*, 6387633. [CrossRef]
28. Joshi, Y.; Rahman, Z. Predictors of young consumer's green purchase behavior. *Manag. Environ. Qual. Int. J.* **2016**, *27*, 452–472. [CrossRef]
29. Hortaçsu, A.; Madanizadeh, S.A.; Puller, S. Power to choose? an analysis of consumer inertia in the residential electricity market. *Nber Work. Pap.* **2015**, *9*, 192–226.

30. Dong, L.-J.; Tang, Z.; Li, X.-B.; Chen, Y.-C.; Xue, J.-C. Discrimination of mining microseismic events and blasts using convolutional neural networks and original waveform. *J. Cent. South Univ.* **2020**, *27*, 3078–3089. [CrossRef]
31. Dong, L.; Zhou, Y.; Deng, S.; Wang, M.; Sun, D. Evaluation methods of man-machine-environment system for clean and safe production in phosphorus mines: A case study. *J. Cent. South Univ.* **2021**, *28*, 3856–3870. [CrossRef]